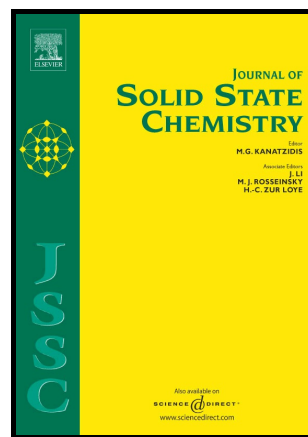


Author's Accepted Manuscript

Two Supramolecular Complexes Based on Polyoxometalates and Co-EDTA Units via Covalent connection or Non-covalent Interaction

Chunlin Teng, Hanxi Xiao, Qing Cai, Jianting Tang, Tiejun Cai, Qian Deng.



www.elsevier.com/locate/jssc

PII: S0022-4596(16)30329-2
DOI: <http://dx.doi.org/10.1016/j.jssc.2016.08.021>
Reference: YJSSC19501

To appear in: *Journal of Solid State Chemistry*

Received date: 19 May 2016
Revised date: 15 August 2016
Accepted date: 17 August 2016

Cite this article as: Chunlin Teng, Hanxi Xiao, Qing Cai, Jianting Tang, Tiejun Cai and Qian Deng., Two Supramolecular Complexes Based on Polyoxometalates and Co-EDTA Units via Covalent connection or Non-covalent Interaction, *Journal of Solid State Chemistry*, <http://dx.doi.org/10.1016/j.jssc.2016.08.021>

This is a PDF file of an unedited manuscript that has been accepted for publication. As a service to our customers we are providing this early version of the manuscript. The manuscript will undergo copyediting, typesetting, and review of the resulting galley proof before it is published in its final citable form. Please note that during the production process errors may be discovered which could affect the content, and all legal disclaimers that apply to the journal pertain.

Two Supramolecular Complexes Based on Polyoxometalates and Co-EDTA Units via Covalent connection or Non-covalent Interaction

Chunlin Teng^[a], Hanxi Xiao^[a], Qing Cai^[b], Jianting Tang^[a], Tiejun Cai^[a] and Qian Deng^{*[a]}

[a] Key Laboratory of Theoretical Organic Chemistry and Functional Molecule for Ministry of Education, Hunan University of Science and Technology, Xiangtan 411201, China

[b] Chemistry Department, City University of New York, New York, NY 10016, USA

E-mail: dengqian10502@163.com

Abstract:

Two new 3D network organic-inorganic hybrid supramolecular complexes $\{[\text{Na}_6(\text{CoEDTA})_2(\text{H}_2\text{O})_{13}] \cdot (\text{H}_2\text{SiW}_{12}\text{O}_{40}) \cdot x\text{H}_2\text{O}\}_n$ (1) and $[\text{CoH}_4\text{EDTA}(\text{H}_2\text{O})]_2(\text{SiW}_{12}\text{O}_{40}) \cdot 15\text{H}_2\text{O}$ (2) (H_4EDTA = Ethylenediamine tetraacetic acid) have been successfully synthesized by solution method, and characterized by infrared spectrum (IR), thermogravimetric-differential thermal analysis (TG-DTA), cyclic voltammetry (CV) and single-crystal X-ray diffraction (XRD). Both of the complexes are the supramolecules, but with different linking mode, they are two representative models of supramolecule. complex (1) is a 3D infinite network supramolecular coordination polymer with a rare multi-metal structure of sodium-cobalt-containing, which is mainly linked through coordinate-covalent bonds. While complex (2) is normal supramolecule, which linked by non-covalent interactions, such as H-bonding interaction, electrostatic interaction and van der Waals force. Both of complex (1) and (2) exhibit good catalytic activities for catalytic oxidation of methanol, when the initial concentration of methanol is $3.0 \text{ g} \cdot \text{m}^{-3}$, flow rate is $10 \text{ mL} \cdot \text{min}^{-1}$, and the quantity of catalyst is 0.2 g, for complex (1) and complex (2) the maximum elimination rates of methanol are 85% ($150 \text{ }^\circ\text{C}$) and 92% ($120 \text{ }^\circ\text{C}$), respectively.

Keywords: Polyoxometalates, Organic-inorganic hybrid, Supramolecule, Crystal

structure, Catalytic activity

1. Introduction

At present, the research into polyoxometalates (POMs) is a hot topic in many scientific fields, mainly because of their controllable shape, size, composition, structural diversity, and most importantly, their vast range of promising properties, such as photochromism [1], magnetism [2], efficient adsorbents [3], macromolecular crystallography [4], medicine [5], catalysis [6] explain the growing interest in POMs by the scientific community. Several strategies have been considered to modify POMs while retaining their structural integrity, intrinsic properties, and facilitating their implementation into extended structures. The mostly extended POMs are generalized as polyoxometalate-based open frameworks (POM-OFs) by Miras and Cronin [7]. POM-OFs are extended architectures incorporating metal-oxide cluster units and comprise an emergent family of materials with a large diversity of topologies, structural flexibility and functionality at the nanoscale. In addition, not only do POM-OFs present a wide range of configurable structures, but also have a vast array of physical properties. POM-OFs family can be classified two types: (i) inorganic–organic hybrids: inorganic and organic structural elements co-exist within a single phase; (ii) inorganic-inorganic hybrids: POMs exists solely with inorganic structural elements in a single phase. Much of the focus in polyoxometalate area during the last few years has been on hybrid frameworks especially for organic–inorganic hybrids, which are of interest for potential applications in catalysis, separations and sensors. To date, many POM-based inorganic–organic hybrid compounds constructed from metal ions and rigid/flexible ligands have been reported [8-13]. But the design and synthesis of inorganic–organic hybrids based on POMs with various topologies are still challenging and interesting tasks in modern inorganic chemistry. Besides choosing the appropriate POM and rigidity/flexibility of organic ligands [14] as the starting materials, it is very important to control other parameters such as the pH value [15], the possible utilization of metal [16], reaction temperature [17] and molar ratios of starting materials [14], which may just a little deviation will make a great difference.

POM-based inorganic–organic hybrids represent the interface between two chemistries of inorganic and organic compounds with significant contributions to the field of material science. Such hybrid materials may provide additional and/or enhanced functions and properties as a result of synergistic interactions between the inorganic and organic components, which reflect the properties of the various ‘modular’ molecular inputs. These POMs based inorganic–organic hybrids can be classified conveniently into two main classes, according to the main chemical interactions between the inorganic (POM) and organic/metal - organic components. Type I inorganic-organic hybrids refer to the situation where weak supramolecular interactions (e.g. non-covalent interactions such as hydrogen bonding, electrostatic, van der Waals force and so on) are the dominant interactions between two components; whereas the hybrids can be categorized as type II when stronger interactions of coordinative covalent bonds are dominant, in which POMs leads itself to play the linkages role as inorganic ligand. Taking advantage of these interactions, many interesting supramolecular architectures with high dimensionality and connectivity can be obtained. Usually, the compounds with infinite supramolecular architectures formed by non-covalent weak interactions and/or coordinative covalent bonds belong to supramolecules and coordination polymers, respectively. The coordination polymers are coordination compounds with repeating coordination entities extending in 1, 2, or 3 dimensions [18]. Many coordination polymers not only present coordinative covalent bonds, but also have a vast array of weak supramolecular interactions. Thus this kind of coordination polymers also can be assigned to the category of supramolecule. However, there is an unfavourable lack of investigation on the interactions (non-covalent interactions or covalent connections) between POM and metal–organic units [19]. In comparison with other inorganic–organic coordination polymers, the rational design and assembly of POM-based supramolecules, especially covalent connection, remains an arduous task for polyoxometalate chemists.

In this paper, we choose the same starting materials of Keggin polyanions

$[\text{SiW}_{12}\text{O}_{40}]^{4-}$, cobalt ions and H_4EDTA molecule, but different parameter of pH value, obtaining supramolecules with different interactions (non-covalent interactions and/or covalent connections) between inorganic and organic units. The structures and properties of two hybrids have been detailed investigated. The two complexes show excellent catalytic activities for catalytic oxidation of methanol.

2. Experimental

2.1. Materials and methods

All reagents were purchased commercially and used without further purification.

The crystal structures of complex (1) and (2) were determined with a Bruker Smart Apex II CCD area detector single-crystal diffractometer (Bruker, Germany) with graphite-monochromatized $\text{MoK}\alpha$ ($\lambda = 0.71073 \text{ \AA}$) radiation by the ψ - ω scan method. Infrared spectra (IR) were recorded as KBr pellets on a Perkin-Elmer FTIR-2000 spectrometer. Thermogravimetric differential thermal (TG-DTA) data of the samples were obtained on a WCT-1D instrument (Beijing optical instrument factory, Beijing, China) from room temperature to $900 \text{ }^\circ\text{C}$ under air atmosphere, heating-rate was $10 \text{ }^\circ\text{C}\cdot\text{min}^{-1}$. Cyclic voltammetry (CV) curves were tested on Electrochemical work station CH1760C of Shanghai Chen-Hua Instrument at different scan rates, glassy carbon electrode, platinum electrode and calomel electrode been used as the working electrode, auxiliary electrode and reference electrode respectively. UV-vis spectra were measured on a TU-1810 spectrophotometer (SHIMADZU, Japan).

2.2. Synthesis

Synthesis of CoEDTA: 6.269 g (21.45 mmol) of H_4EDTA was dissolved in 500 mL water, heated to boiling, then 6.867 g (23.6 mmol) $\text{Co}(\text{NO}_3)_2\cdot 6\text{H}_2\text{O}$ was slowly added. The mixed solution kept boiling and stirred for 30 min, filtered. Then the filtrate was heated to appearing white precipitation in the solution. The precipitation was dried at $60 \text{ }^\circ\text{C}$ to obtain purple powder CoEDTA, it was about 91.1 % yield (based on H_4EDTA).

Synthesis of complex (1): 1.439 g (0.5 mmol) $\text{H}_4\text{SiW}_{12}\text{O}_{40}\cdot n\text{H}_2\text{O}$ and 0.2071 g

(0.59 mmol) CoEDTA was dissolved in 10 mL deionized water. The mixture was kept at 80 °C for 30 min, cooled to room temperature, and the solution pH was adjusted to 1.95 by the addition of 5 mol·L⁻¹ NaOH and 1:1 (V:V) H₂SO₄. Then the mixture was kept at 60 °C stirring for 30 min. The warm solution was filtered, kept in dry dark cultivation cabinet. The pure regular purple cube crystals were obtained in ambient conditions for three weeks. Yield: 65.4 % (based on W).

Synthesis of complex (2): the synthesis method of complex (2) is similar to (1), except pH=0.41, then pure red hexahedral crystals were obtained after about two weeks. Yield: 70.2 % (based on W).

2.3. X-ray Structure Determination

The reflection intensities of complex (1) and (2) were collected on a Bruker Smart Apex II CCD area detector single-crystal diffractometer with graphite monochromated Mo-K α radiation ($\lambda = 0.71073 \text{ \AA}$) at 123K in the range of $3.03 < \theta < 25.10$ and at 293 K in the range of $1.62 < \theta < 25.10$, respectively. Multiscan absorption corrections were applied with the SADABS program [20]. All non-hydrogen atoms were finally refined with anisotropic displacement parameters. The structures were solved by direct methods and refined by full-matrix least-squares on F^2 using the Shelxtl-97 program package [21]. All hydrogen atoms of the two crystals water were added by different Fourier methods while other hydrogen atoms were finally refined as a riding mode using the default Shelxtl parameters.

The detailed crystal data and structure refinement details for complex (1) and (2) are summarized in Table 1. Selected bond lengths, bond angles and hydrogen bonds are given in supplementary material. Crystallographic data for the structures reported in this paper have been deposited in the Cambridge Crystallographic Data Center. CCDC ID of the complex(1) and (2) are 1059325 and 1046792 respectively.

Table 1. Crystal data and refinement details for complex(1) and (2)

	complex (1)	complex (2)
Empirical formula	{[Na ₆ (CoEDTA) ₂ (H ₂ O) ₁₃] ·(H ₂ SiW ₁₂ O ₄₀)·xH ₂ O}n	[CoH ₄ EDTA(H ₂ O)] ₂ (SiW ₁₂ O ₄₀)·15H ₂ O
Formula weight	15698.92	7531.63
Temperature	123K	293K

Dc/(g·cm ⁻³)	3.555	2.655
Crystal system	Monoclinic	Triclinic
Space group	P2 ₁ /n	P $\bar{1}$
a / Å	a = 15.4691(6),	a = 13.0101(5),
b / Å	b = 29.3237(13),	b = 14.5594(6),
c / Å	c = 16.5389(7)	c = 19.4444(8)
α / (°)	$\alpha=90$,	$\alpha=81.734(3)$,
β / (°)	$\beta=102.1600(10)$,	$\beta=75.230(4)$,
γ / (°)	$\gamma=90$	$\gamma=85.989(3)$
Volume/Å ³	7333.9(5)	3522.3(3)
Z	1	1
M μ (MoKa), mm ⁻¹	19.348	20.102
Colour	purple	red
F(0 0 0)	7056.0	3378.0
Limiting indices	-18<=h<=18, -35<=k<=34, -19<=l<=19	-15<=h<=15, -17<=k<=13, -23<=l<=20
R ₁ [I>2 σ (I)] ^a	0.0524	0.0682
wR ₂ [I>2 σ (I)] ^b	0.1415	0.1983
Goof(S)	1.089	1.025
Parameters	1072	990
Refl. unique	12986	12469
Crystal size / mm	0.2×0.15×0.16	0.23×0.2×0.16
θ Range(°)	3.03 -25.10	1.62-25.10
$\Delta\rho$ fin (max / min), e Å ⁻³	4.314 /-2.986	2.382/ -3.244

2.4.2. Catalytic Activity

Catalytic reactions were carried out in a continuous-flow fixed-bed micro-reactor (Fig. 1). The catalytic properties of complexes were tested by eliminating the methanol. 0.2g complex was loaded in the catalytic reaction tube (ϕ /8 mm; L/200 mm) as catalyst. The simulacrum of polluted air containing reaction substrate of methanol gas was prepared by bubbling clean air into a container filled with reaction substrate and diluting the gas with clean dry air. The initial concentration of reaction substrate was dominated by adjusting the flow velocity of the bubbling gas and dilution air. The feed gas flow through the reactor, the catalytic elimination reaction carried on at different temperature, which controlled by a thermostat. The substrate concentration was detected by online gas chromatograph (GC-102M, FID detector) once in every 10 min until the concentration unchanged which means the reaction reaches balance. The

inorganic products of the effluent gases were monitored by a PdCl_2 [0.2 (wt-%)] solution and saturated lime-water solution.

Blank experiment was carried out without the catalysts, and control experiment was tested with $\text{H}_4\text{SiW}_{12}\text{O}_{40}$ as catalyst.

In this research, elimination rate of the substrate was adopted to evaluate the catalytic activity of the samples. The elimination rate was calculated by the following function:

$$X\% \text{ (elimination rate)} = \frac{C_0 - C}{C_0} \times 100\%$$

Where C_0 is the initial concentration of substrates, C represents the residual concentration of the substrate after catalytic reaction.

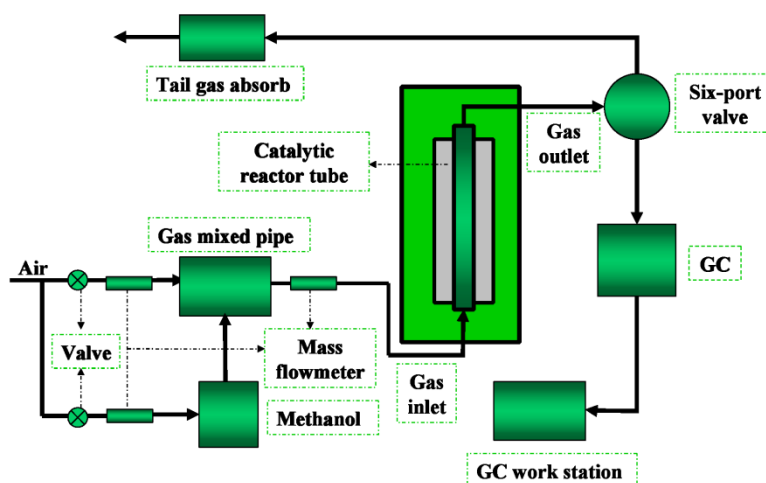


Fig. 1. Continuous flow catalytic schematic diagram.

3. Results and discussion

3.1. Synthesis

Many POM-based compounds with diverse structural architectures have been synthesized using solution method. In most cases, the reaction mechanisms remain elusive and the control and prediction of crystal structures is very difficult, because the architecture of the final product depends on the interplay of starting materials, material ratios, pH value, template, reaction temperature and pressure, et al. As is

well-known, the pH of the reaction system generally has a decisive impact on the formation of the final product in polyoxometalate chemistry, which has an influence on the structural control of the self-assembly process. Complexes (1) and (2) have been synthesized with same method but for different pH value (pH \approx 1.95 for 1 and pH \approx 0.41 for 2) froming two unique molecules. In addition, we also performed many experiments with similar synthetic conditions but with different pH values getting different complex, but perfect single crystal could not be obtained. Therefore, the pH values have been adjusted to the conditions required to obtain the products.

Based on the below-mentioned description, the two complexes possess big structure difference, which are caused by the value of pH. Higher pH in synthesis system of complex (1), provides more Na⁺ ions, that may be useful to build covalent connections and complex (1) with lower acidity than complex (2).

3.2. Crystal structure of complexes 1 and 2

The complex (1) is an infinite supramolecular coordination polymer, which is main linked by many coordinativecovalent bonds with Na⁺ ions as linker. The asymmetric structure unit of complex (1) is shown in Fig. 2a. It consists a Keggin type of [SiW₁₂O₄₀]⁴⁻ anion, a large cation [Na₆(CoEDTA)₂(H₂O)₁₃]²⁺ and many crystalline water molecules. In this rigid POM assemblies, the components are not only held together by the supramolecular interactions, but typically by coordinative bonds. The coordination entities of asymmetric structure units repeating extend forming supramolecular coordination polymers with three- dimension.

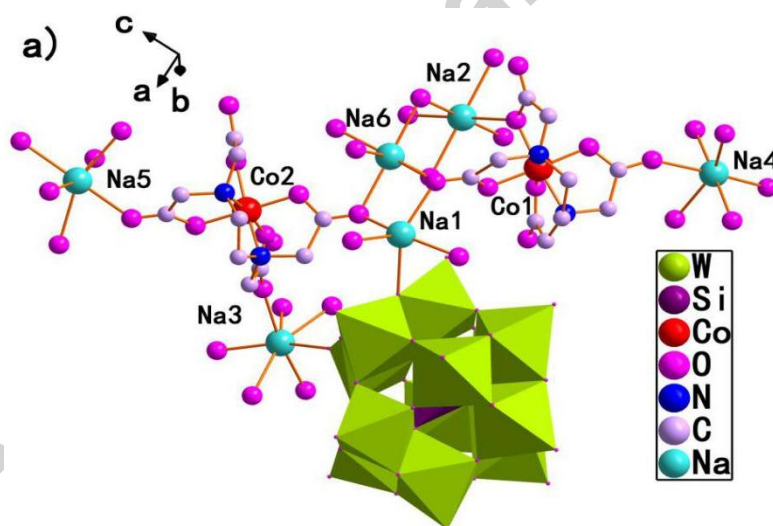
The [SiW₁₂O₄₀]⁴⁻ is a normal α -Keggin structure consisted by a center SiO₄ tetrahedron and twelve corner or edge sharing WO₆ octahedra, which is T_d symmetry. The Si-O_a(central oxygen) distance in the range of 1.610(9)-1.634(9) Å, and the O_a-Si-O_a angle is in the range of 108.4(4)-110.7(5)°, suggesting the formation of a micro-distortion tetrahedron. The W-O_d(terminal oxygen), W-O_a, W-O_{b/c}(bridge oxygen) distances fall in the ranges of 1.686(10)-1.711 Å, 2.316(9)-2.373(9) Å and 1.884(9)-2.356(8) Å, respectively, and the O-W-O angle of the axial direction is in the range of 72.4(3)-173.2°, indicating that WO₆ are distorted octahedrons. The

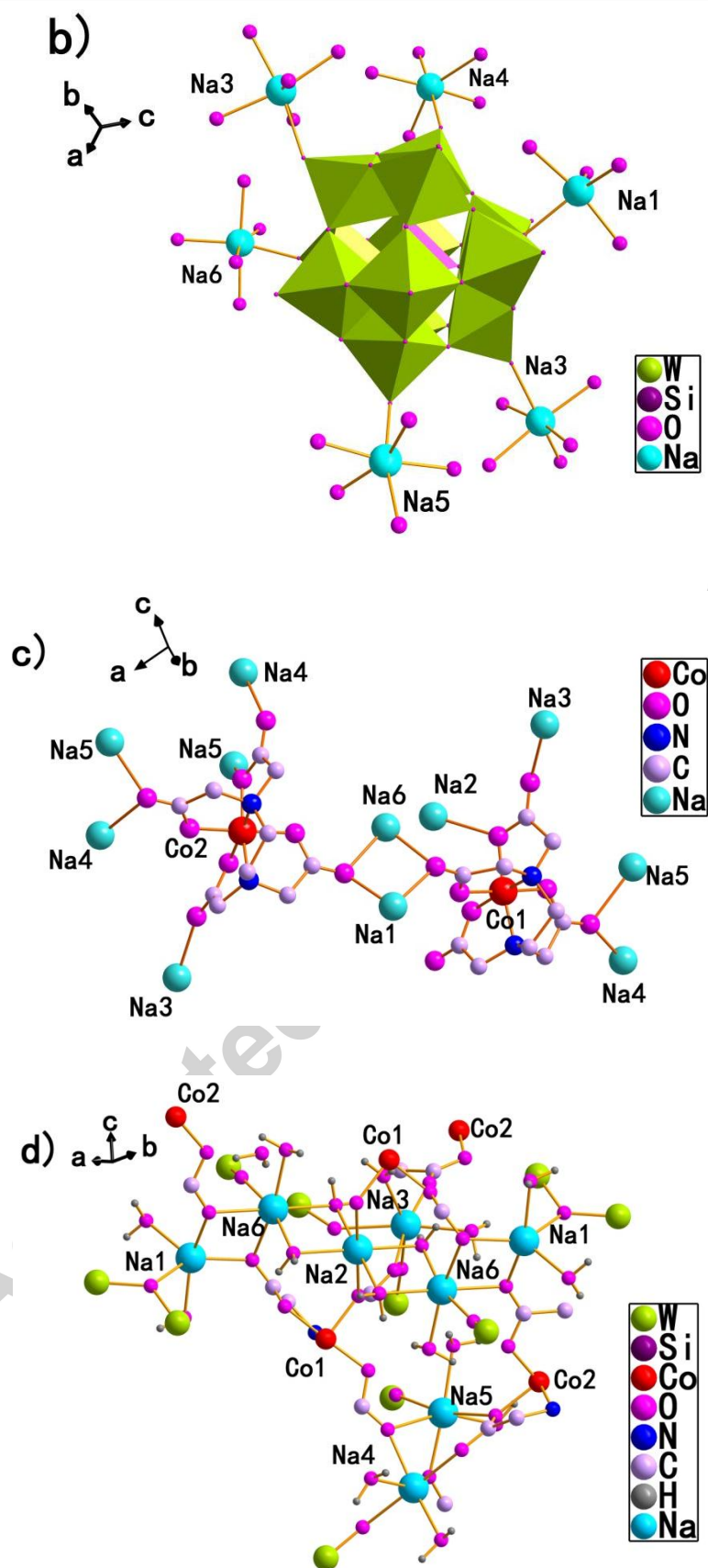
$[\text{SiW}_{12}\text{O}_{40}]^{4-}$ anions in complex (1) are not independent, but as inorganic ligand linking with metal - organic (Co-EDTA) units through Na^+ ions by coordinative bonds, forming six-coordinated heteropoly anions. (Fig. 2b). This means the POMs are incorporated into the framework as integral components in the scaffold, and are linked into extended three-dimensional structures through metals. According to Cui and Xu model [22], the connectivity mode of complex (1) is mostly similar with d-type that an organic linker via metal (M) sites outwith the POM cluster connects with POM, which were named as POM-metal-organic frameworks. In complex (1), each Co^{2+} ion adopts six-coordinated octahedral $\{\text{CoN}_2\text{O}_4\}$, which is coordinated by four carboxyl oxygen atoms and two nitrogen atoms of amino groups of H_4EDTA , forming $[\text{CoEDTA}]$ chelate. The bond length of Co-O/N is in the range of 1.865(9)-1.937(11) Å, which suggests a distorted octahedral form. It is worth noting that all the $[\text{CoEDTA}]$ chelates further coordinate with many Na^+ ions, through hydroxy and carbonyl oxygen atoms of carboxyl groups. But the $[\text{CoEDTA}]$ chelates can be divided into two groups of $[\text{Co1EDTA}]$ and $[\text{Co2EDTA}]$, according to the coordinated number of sodium. The $[\text{Co1EDTA}]$ coordinates with six Na^+ ions by three carbonyl oxygen atoms of carboxyl groups and one hydroxy oxygen atom of carboxyl group (Fig. 2c). Thus the coordination behavior of these H_4EDTA ligands in $[\text{Co1EDTA}]$ are described as $\mu_7-\eta^9$ mode [23]. While in $[\text{Co2EDTA}]$ seven Na^+ ions coordinate with four carbonyl oxygen atoms and one hydroxy oxygen atom of carboxyl groups (Fig. 2c), that the chelating mode of $[\text{Co2EDTA}]$ can be described as $\mu_8-\eta^{10}$. That is to say almost all the coordination sites of H_4EDTA have been used, as high-dentate ligand that high-nuclear clusters are formed. To the best of our knowledge, this high-dentate and multi-metal chelating mode of H_4EDTA is quite rare.

In the molecular structure of complex (1) many Na^+ ions are existed, which play an important role to link $[\text{Co1EDTA}]$, $[\text{Co2EDTA}]$ and $[\text{SiW}_{12}\text{O}_{40}]^{4-}$ together, forming a 3D infinite supramolecule (Fig. 2d, e). There are six coordination environments of Na^+ ions in the complex, which are labeled from Na1 to Na6 (Fig. 2d). The coordination situations of six types Na^+ ions are summarized in Table 2. Except Na1 is five-coordinated forming tetragonal pyramid, all other types of Na^+ ions are

six-coordinated with octahedral structure. It is caused for that Na1 coordinates with $O_{b/c}$ atom of $[\text{SiW}_{12}\text{O}_{40}]^{4-}$, but others with O_d , Na1 is more near heteropoly anion $[\text{SiW}_{12}\text{O}_{40}]^{4-}$, that with bigger space steric hindrance, so it only forms five instead of six coordination. In addition, it's worth noting that all the Na^+ ions coordinate with $[\text{SiW}_{12}\text{O}_{40}]^{4-}$ cation except for Na2. Na2 is in the center of the structure unit, far from the $[\text{SiW}_{12}\text{O}_{40}]^{4-}$ cation, coordinates with two EDTA ligands in axial direction of the octahedron and four water molecules on the plane of the octahedron, forming quite symmetric configuration, which is every useful to stable the complex. The Na – O bond length is in the range of 2.273(11) ~ 2.538 (12) Å, which is in a reasonable scope and consistent with the values reported in the literature [24]. Na^+ ions play key function in constructing this 3D infinite supramolecule.

It's worth noting that not only the coordinative bonds but also a great number of non-covalent bonds of hydrogen bonds (Table S3) between organic ligands, lattice water molecules and $[\text{SiW}_{12}\text{O}_{40}]^{4-}$ anions help to build supramolecular structure of complex (1).





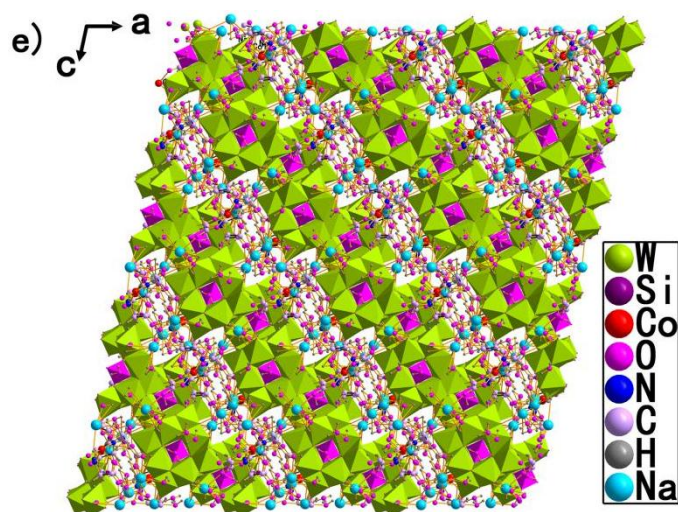


Fig. 2. (a) The ball-and-stick representation of the asymmetric structure unit of complex (1). (b) The coordination model of $[\text{SiW}_{12}\text{O}_{40}]^{4-}$ anion. (c) The chelate model of H_4EDTA . (d) The coordination model of Na^+ ions. (e) The three-dimensional structure of complex (1) along $[010]$ direction. (The hydrogen atoms of (a), (b) and (c) have been omitted for clarity)

Table 2. The coordination situations of six types Na^+ ions in complex (1)

Type of Na^+ Coordination Situation	Coordination			
	Number	H_2O	EDTA	$[\text{SiW}_{12}\text{O}_{40}]^{4-}$
Na1	5	2	2	1($\text{O}_{b/c}$)
Na2	6	4	2	0
Na3	6	2	2	2(O_d)
Na4	6	2	3	1(O_d)
Na5	6	2	3	1(O_d)
Na6	6	3	2	1(O_d)

The molecular structure of complex (2) is shown in Fig. 3a. The single-crystal X-ray analysis reveals that complex (2) is a common 3D supramolecule, which is mainly assembled by non-covalent interactions of hydrogen bonds, electrostatic interaction and van der Waals force. Complex (2) is constructed from one $[\text{SiW}_{12}\text{O}_{40}]^{4-}$ anion, two cations of $[\text{CoH}_4\text{EDTA}(\text{H}_2\text{O})]^{2+}$ and fifteen water molecules. On the crystallography these constituents are independent, while on the molecular level they are an integrated, which are mainly assembled by non-covalent bonds of hydrogen bonds and electrostatic interaction forming charge-transfer supramolecular hybrid

involving organic donors and inorganic acceptors.

The $[\text{SiW}_{12}\text{O}_{40}]^{4-}$ anion in complex (2) is same as that in complex (1), which is Keggin type but with a little distortion for the interactions between $[\text{SiW}_{12}\text{O}_{40}]^{4-}$ anion and metal-organic cations. But $[\text{SiW}_{12}\text{O}_{40}]^{4-}$ anion in complex (2) is independent without directly coordinating with other metal ion.

In complex (2) Co^{2+} ions show six-coordinated octahedral geometry, which coordinated through three carboxyl oxygen atoms, two nitrogen atoms of amino groups of H_4EDTA and one oxygen atom of a water molecule, forming $[\text{CoH}_4\text{EDTA}(\text{H}_2\text{O})]^{2+}$ chelates (Fig. 3a). The bond length of Co-O/N is in the range of 1.885(7)-1.975(8) Å, which suggests the chelates with distorted octahedral form.

There are a lot of intramolecular and intermolecular hydrogen bonds in complex (2) (Fig. 3b), which play an important role in consolidating the crystal architecture and making the complex form 3D supermolecular architecture (Fig. 3c). For example: intramolecular hydrogen bonds of C(8) -- H(8B) ... O(27), $d(\text{C} \cdots \text{O}) = 3.18(3)$ Å, $\angle \text{C} \cdots \text{O} = 165^\circ$ and C(5) -- H(5B) ... O(2), $d(\text{C} \cdots \text{O}) = 3.23(3)$, $\angle \text{C} \cdots \text{O} = 134^\circ$; intermolecular hydrogen bonds of O(67) -- H(67B) ... O(43), $d(\text{O} \cdots \text{O}) = 2.68(5)$ Å, $\angle \text{O} \cdots \text{O} = 164^\circ$ and O(68) -- H(68D) ... O(52), $d(\text{O} \cdots \text{O}) = 2.61(6)$ Å, $\angle \text{O} \cdots \text{O} = 110^\circ$. These significant non-covalent interactions of hydrogen bonds make numerous metal - organic cations in complex (2) link together forming intersected lattices, which are occupied by $[\text{SiW}_{12}\text{O}_{40}]^{4-}$ counterions (Fig. 3c). Therefore, H-bonds play an important role in stabilizing the ultimate structure.

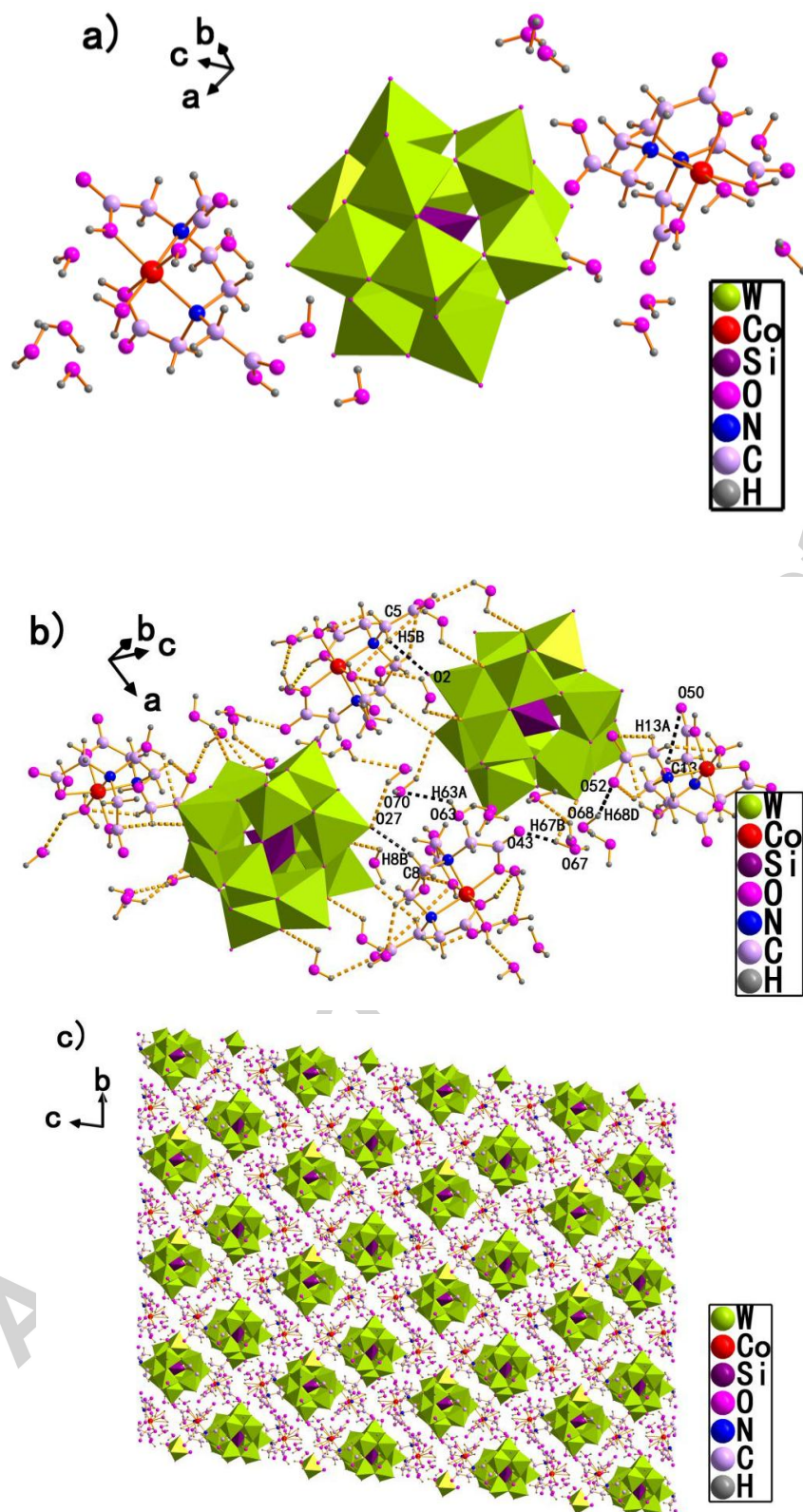


Fig. 3. (a) The ball-and-stick representation of the building block of complex (2). (b) The model of hydrogen bonds in complex (2). (c) The three-dimensional structure of complex (1) along [100] direction.

Complex (2) and many others reported compounds in the literatures are attributed

to conventional supramolecule, which are constructed by hydrogen bonding, electrostatic, van der Waals force and/or $\pi\cdots\pi$ stacking interactions, et al. While complex (1) is special, in addition to above supramolecular forces, coordinative covalent bonds are existed, which promote the high-nuclear infinite supramolecule forming, and belongs to supramolecular coordination polymer. Based on the above-mentioned description, the interactions between POMs and metal-organic units play an important role in forming the ultimate structures. Further insight into the nature of the two complexes, the coordination modes of Keggin-type polyanions also have significant effects on the final structure and stability of complex. The Keggin-type polyanions can coordinate to metal ions in a variety of coordination modes such as non-covalent interactions and/or covalent connections to form many attractive compounds with different dimensions [19, 25]. In complex (1), the polyanions play two roles, one acts as a bridge (six-dentate bridge) to link metal centers from different metal-organic sheets, and two as a counterion to co-crystallize in the structure forming a 3D framework. In complex (2), polyanion acts as counterion and occupy the space that is formed by metal-organic units (Fig. 3c).

3.3. IR spectrum

The IR spectra of complex (1), (2) and $\text{H}_4\text{SiW}_{12}\text{O}_{40}$ are shown in Fig. 4. The infrared spectra of complexes exhibit four characteristic peaks of the Keggin anions in the low-wave number region ranging 700 cm^{-1} to 1100 cm^{-1} . The bands at 1019 cm^{-1} , 978 cm^{-1} , 925 cm^{-1} , 798 cm^{-1} for complex (1) and 1017 cm^{-1} , 976 cm^{-1} , 933 cm^{-1} , 816 cm^{-1} for complex (2) are corresponding to $\square(\text{W}-\text{O}_d)$, $\square(\text{Si}-\text{O}_a)$, $\square(\text{W}-\text{O}_b)$ and $\square(\text{W}-\text{O}_c)$ stretching vibration respectively [26-27]. Comparing with their parent heteropolyacid $\text{H}_4\text{SiW}_{12}\text{O}_{40}$ ($\text{W}-\text{O}_d$: 1018 cm^{-1} , $\text{Si}-\text{O}_a$: 980 cm^{-1} , $\text{W}-\text{O}_b$: 925 cm^{-1} , $\text{W}-\text{O}_c$: 778 cm^{-1}), which have some blue-shift. The results suggest that metal-organic ligands interact with heteropolyacid anion leading to the change of charge density around anion, which transform the force constant of $\text{W}-\text{O}_{b/c}$. Meanwhile the results validate there still remains Keggin framework in complexes.

The peaks at 3446 cm^{-1} ($\nu(\text{O}-\text{H})$), 2991 cm^{-1} ($\nu(-\text{CH}_2)$), 1655 cm^{-1} ($\nu(\text{C}=\text{O})$), 1362

cm^{-1} , 1208 cm^{-1} (δ (C-H)), 1174 cm^{-1} (ν (C-N)) for complex (1) and 3435 cm^{-1} (ν (O-H)), 3000 cm^{-1} (ν (-CH₂)), 1635 cm^{-1} (ν (C=O)), 1460 cm^{-1} , 1362 cm^{-1} (δ (C-H)), 1222 cm^{-1} (ν (C-N)) for complex (2) are contributed to the characteristic peaks of H₄EDTA ligand.

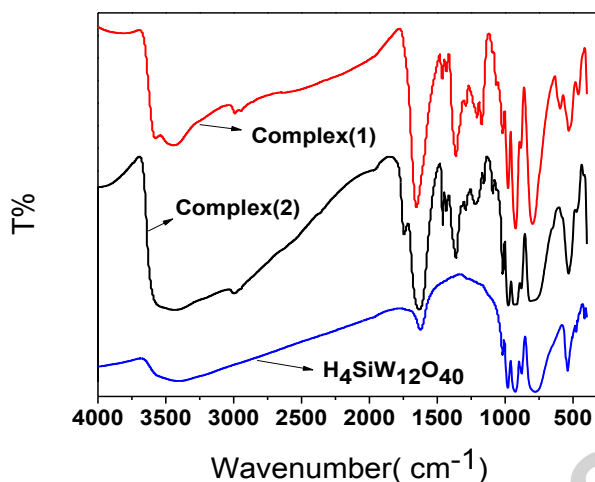


Fig. 4. The IR spectra of complex (1), (2) and H₄SiW₁₂O₄₀

3.4. Thermogravimetric-differential thermal analysis

TG-DTA curves of complex (1) and (2) are presented in Fig. 5(a), (b) respectively, which were tested in the air atmosphere with heating rate of $10 \text{ }^{\circ}\text{C}\cdot\text{min}^{-1}$ from $25 \text{ }^{\circ}\text{C}$ to $900 \text{ }^{\circ}\text{C}$.

The TG-DTA test of complex (1) shows five weight loss steps, accompanied by endothermic and exothermic peaks (Fig. 5a). The first weight loss step occurs from $25 \text{ }^{\circ}\text{C}$ to $110 \text{ }^{\circ}\text{C}$, the loss rate is 5.56% , accompanied with two endothermic peaks at around $64 \text{ }^{\circ}\text{C}$ and $104 \text{ }^{\circ}\text{C}$, corresponding to the remove of the absorbed and some uncoordinated crystallization water molecules [24]. The second to fourth steps of weight loss appear in $200 \text{ }^{\circ}\text{C} \sim 700 \text{ }^{\circ}\text{C}$, the whole loss rate is 14.09% , accompanied by some exothermic peaks at around $265 \text{ }^{\circ}\text{C}$, $420 \text{ }^{\circ}\text{C}$, $506 \text{ }^{\circ}\text{C}$, $580 \text{ }^{\circ}\text{C}$ and $634 \text{ }^{\circ}\text{C}$, respectively, which are caused by the decomposition of the metal - organic components in the hybrid complex. The fifth weight loss is 1.65% from $760 \text{ }^{\circ}\text{C}$ to $900 \text{ }^{\circ}\text{C}$, assigned to the decomposition of heteropolyanion $[\text{SiW}_{12}\text{O}_{40}]^{4-}$, accompanying with three endothermic peaks at around 720°C , $773 \text{ }^{\circ}\text{C}$ and $830 \text{ }^{\circ}\text{C}$ in DTA curve. The

final residue may be a mixture of SiO_2 , WO_3 , CoO and Na_2O . The weight loss of the whole process is 21.3%, which is agree with the calculated value (17.89%) after getting rid of the absorb water.

The TG-DTA curves of complex (2) are shown in Fig. 5b. The TG curve of complex (2) exhibits four weight loss steps, accompanied by endothermic and exothermic peaks in DTA. The former two steps of weight loss appear in room temperature to 200 °C, with the whole weight loss of 8.55 %, accompanied with two concomitant endothermic peaks at around 84 °C and 135 °C, which are attributed to the loss of the absorbed water and no-coordinated crystal water molecules. The last two steps of weight loss appear in range of 200 °C ~ 700 °C, the whole loss rate is 7.78 %, accompanied with a steamed bread exothermic peak (around 500 °C) and a sharp exothermic peak (590 °C), which are assigned to the decomposition of metal-organic cations and heteropolyanion of $[\text{SiW}_{12}\text{O}_{40}]^{4-}$, respectively. The final residue is purple, which may be a mixture of WO_3 , CoO and SiO_2 . In the whole decomposition process of complex(2), the weight loss rate is 16.33 %, and the calculated value is 19.95 %. Thus the TG analysis results of complex (2) support its chemical composition.

The thermal decomposition temperatures of complex (1) and (2) are all higher than 200°C in air under atmospheric pressure, showing a higher thermal stability. Comparing the maximum decomposition temperatures of them, complex (1) is much higher than complex (2), which may due to that covalent POM-based hybrid. Compared with the non-covalent hybrids, covalent links enhance the interaction between the inorganic and organic components, resulting in the stability of the hybrid improved [19].

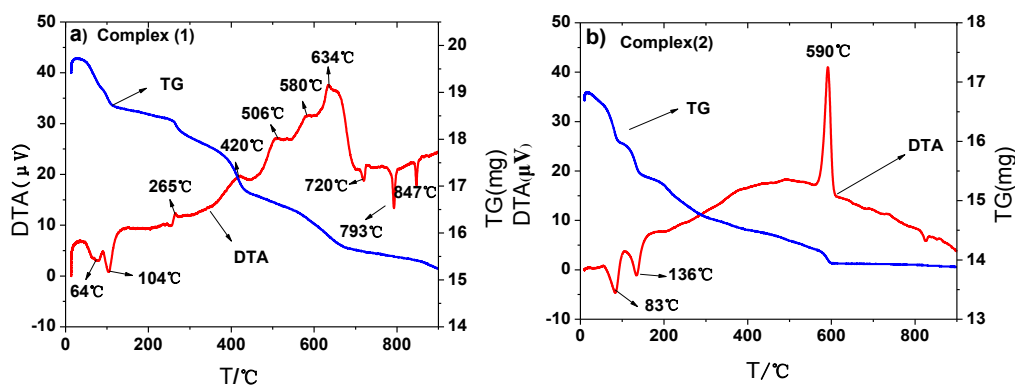


Fig. 5. The TG-DTA curves of complex (1) (a) and (2) (b)

were recorded under air atmosphere

3.5. Cyclic Voltammetry

Fig. 6 shows cyclic voltammograms of complex (1) and (2) in 1 mol·L⁻¹ HCl water solution, by controlled-potential in the range of -0.6 V - 0.1 V at different scan rates.

The redox peaks of I-I', II-II' and III-III' for complex (1) at -0.49 V / -0.53 V, -0.32 V / -0.37 V, -0.11 V / -0.16 V, respectively, with corresponding peak separations ΔE_p of 0.04 V, 0.05 V, 0.05 V. For complex (2) the redox peaks of I-I', II-II' and III-III' at -0.50 V / -0.53 V, -0.32 V / -0.38 V, -0.11 V / -0.16 V, respectively, with corresponding ΔE_p of 0.03 V, 0.04 V, 0.05 V. It can be seen that complex (1) and (2) show the similarly CV curves, both have three pairs symmetrical redox peaks and the redox potentials are very close, which due to that the reactions on the electrode are attributed to W redox of [SiW₁₂O₄₀]⁴⁻. The redox peaks I-I', II-II' and III-III' are assigned to 1-, 1-, 2- electrons reversible redox process, and accompany the protonic process [28]: $\alpha\text{-SiW}_{12}\text{O}_{40}^{4-} + e^- = \alpha\text{-SiW}_{12}\text{O}_{40}^{5-}$, $\alpha\text{-SiW}_{12}\text{O}_{40}^{5-} + e^- = \alpha\text{-SiW}_{12}\text{O}_{40}^{6-}$, $\alpha\text{-SiW}_{12}\text{O}_{40}^{6-} + 2e^- + 2\text{H}^+ = \alpha\text{-H}_2\text{SiW}_{12}\text{O}_{40}^{6-}$.

In complex (1) and (2), the first two pairs redox peaks appear with ΔE_p < 0.059/n (V) and ip_a / ip_c ≈ 1, which suggest reversible redox processes. The third pair redox peaks appears with ΔE_p > 0.059/n (V), but the peaks are symmetrical, ip_a / ip_c ≈ 1 and at different scan rates the potentials of the redox peaks aren't obvious change. The results indicate that this step is a quasi-reversible process [29], which might be due to non-ideal reversible behaviors [30]. Therefore, the two complexes have

reversible redox features.

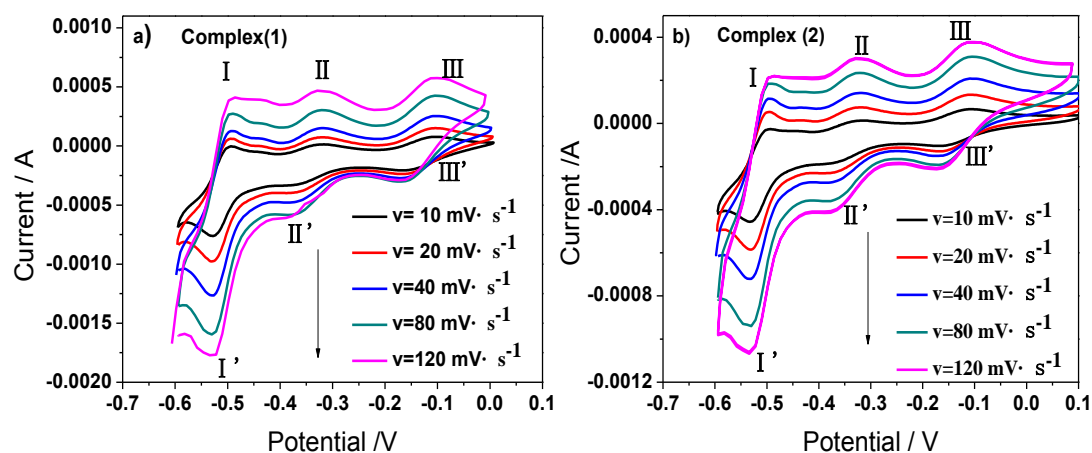


Fig. 6. Cyclic voltammograms of complex (1) (a) and (2) (b) in $1 \text{ mol}\cdot\text{L}^{-1}$ HCl solution at different scan rates of $10 - 140 \text{ mV}\cdot\text{s}^{-1}$, volume: 100 mL , concentration, $1\times 10^{-3} \text{ mol}\cdot\text{L}^{-1}$.

3.6. UV-vis spectrum

The UV-vis spectra of $\text{H}_4\text{SiW}_{12}\text{O}_{40}$, complex (1), (2) and H_4EDTA in solution state are shown in Fig. 7. In the test wavelength range, H_4EDTA only displays a weak absorption with the maximum absorption at 200 nm . While $\text{H}_4\text{SiW}_{12}\text{O}_{40}$, complex (1) and (2) show two strong absorption peaks at around 210 nm and 260 nm , which are the character peaks of heteropolyanion [31]. The strong absorptions at 210 nm and 260 nm are attributed to $\text{O}_d \rightarrow \text{W}$ LMCT (Ligand-to-metal charge transfer) and $\text{O}_{b/c} \rightarrow \text{W}$ charge transfer transition, respectively. The results suggest that after forming organic-inorganic hybrids complex (1), (2) still keep the Keggin structure of heteropolyanions.

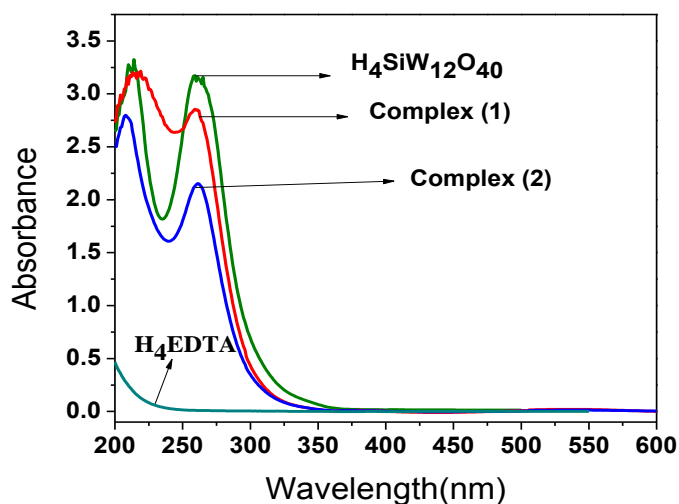


Fig. 7 The UV-vis spectra in aqueous solution for $\text{H}_4\text{SiW}_{12}\text{O}_{40}$, complex (1), (2) and H_4EDTA

3.7. Catalytic performance

Polyoxometalates have available orbitals and strong oxidability which can undergo redox processes without major structural rearrangements. This is the reason that reduced POMs species are often referred to as reservoirs of electrons, a property which is crucial for the catalytic activity of the prepared POM-based materials [7]. The catalytic activities of catalytic oxidation methanol of complex (1) and (2) have been studied, and by comparing the differences between heteropolyacid and organic-inorganic hybrids the effect of ligand/metal-liagand to catalytic activity has been investigated.

Blank experiments show that methanol in a simulacrum of polluted air was not eliminated without complex (1) or (2) as the catalyst. There is no new peak except for that of methanol in gas chromatograph spectra when the catalytic reaction was undergoing, indicating no new organic compounds formed. At the same time, the tail gas made the saturated limewater grow turbid and the color of 0.2% PdCl_2 solution does not change, indicating that CO_2 , but not CO was the product of catalytic elimination of methanol. The controlled trial was done with their parent silicotungstic acid as the catalyst. The temperatures of catalytic reaction were 25 - 200 °C, which are lower than the decomposition temperatures of complex (1) and (2) according to TG-DTA test, that the structures were almost unchanged after catalytic experiments.

The relationships between the elimination rate and temperature are shown in Fig. 8. The reaction was tested at an initial methanol concentration of $3.0 \text{ g}\cdot\text{m}^{-3}$ and a flow velocity of $10 \text{ mL}\cdot\text{min}^{-1}$ over 0.2 g catalyst. At room temperature their elimination rates for methanol are 38%, 39% and 36% for complex (1), (2) and silicotungstic acid, respectively. At relative low temperature, complexes and silicotungstic acid show nearly the same catalytic activity, but at high temperature, the variation trend over complex(1), (2) and $\text{H}_4\text{SiW}_{12}\text{O}_{40}$ are different. With the increase of temperature, the elimination rates increase first, reach their maximum elimination rates: 85% ($150 \text{ }^\circ\text{C}$) for complex (1), 92% ($120 \text{ }^\circ\text{C}$) for complex (2) and 76% ($90 \text{ }^\circ\text{C}$) for $\text{H}_4\text{SiW}_{12}\text{O}_{40}$, respectively. After the maximum elimination temperature with the increase of temperature, the elimination rates of complex (1) and (2) show only slightly declines. But the elimination rate of methanol over $\text{H}_4\text{SiW}_{12}\text{O}_{40}$ has obviously declined when the temperature is above $90 \text{ }^\circ\text{C}$.

Principally, either for the silicotungstic acid or complexes, the heteroatom Si and polyatom W are the highest valence to show the strong oxidizability. In addition heteropolyacids have a cage structure. The special structure creates a lot of gaps that the small organic molecule can get into the heteropolyacids' framework. It is called "false liquid", which has the characteristics of homogeneous catalysis. Therefore both the silicotungstic acid and complexes have the same catalytic abilities to eliminate methanol under relative low temperature. When at high temperature the methanol absorption over silicotungstic acid reduces, lead to the catalytic ability rapidly declines. But after the H_4EDTA ligands interact with $\text{H}_4\text{SiW}_{12}\text{O}_{40}$, forming organic-inorganic hybrid complex, the methanol absorption ability of complex is improved to enhance the catalytic reaction. Thus the elimination rates of complex (1) and (2) still keep a good level at high temperature. On the other hand complex (1) and (2) forms a supramolecular network framework to stabilize their structures, so that complexes still keep high catalytic activity at high temperature.

But comparing the catalytic activities of complex (1) and (2), complex (2) has a slightly higher methanol elimination rate at the same temperature and lower maximum elimination temperature than (1). The mean difference of elimination rate

between (1) and (2) is about 5%. The different catalytic activities of the two complexes may be for the following reasons. It is widely believe that high acidity is advantageous to the oxidation reaction, namely with high catalytic activity. Complex (1) contains many Na^+ ions, that is lower acidity than (2), so catalytic activities of (2) is higher than that of (1). In addition, for the same weight, there are more molecules of (2) compared to (1), so there are more active sites, which could contribute to the higher elimination rate of (2). It may also be attributed to different intensities and numbers of hydrogen bonds of (1) and (2), which show different adsorption ability, affecting the catalytic activity.

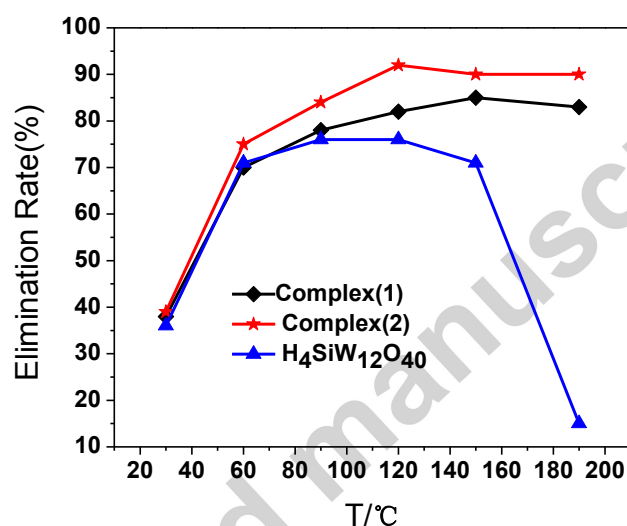


Fig. 8. Elimination rates of methanol for complex (1), (2) and $\text{H}_4\text{SiW}_{12}\text{O}_{40}$

4. Conclusions

In summary, two new 3D network inorganic–organic hybrid supramolecules based on H_4EDTA , metal ions of Co^{2+} and/or Na^+ and Keggin polyanions have been synthesized by solution method. With different pH value the two complexes are formed different supramolecular structure with different connection method between inorganic and organic units. The coordination covalent connections and H-bonding interactions are the main interactions of complex (1) and (2), respectively. In complex (1), polyanions as inorganic ligands and $[\text{CoEDTA}]$ as metal–organic ligands coordinate with Na^+ ions, forming infinite network supramolecule with a rare multi-metal structure of sodium-cobalt-containing. In complex (2) polyanions and $[\text{CoEDTA}]$ are independent on crystallography, but in molecule level they are

interacted by H-bonding interaction, electrostatic interaction and van der waals force, forming supramolecular structure. The result indicates that with different interaction modes of non-covalent interactions and/or covalent connections as connection force in compound can obtain different structure compound. In addition, complex (1) and (2) exhibit good catalytic activities for catalytic elimination of methanol, when the initial concentration of methanol is $3.0 \text{ g}\cdot\text{m}^{-3}$, flow rate is $10 \text{ mL}\cdot\text{min}^{-1}$, and the quality of catalyst is 0.2 g, and the maximum elimination rates of methanol are 85% ($150 \text{ }^\circ\text{C}$) for complex (1) and 92% ($120 \text{ }^\circ\text{C}$) for complex (2), respectively.

Acknowledgments

This work was supported by the Key Laboratory of Theoretical Organic Chemistry and Functional Molecules of Ministry of Education and the Organic Chemistry Key Subject of Hunan Province of China.

References

- [1] R. Dessapt, M. Gabard, M. Bujoli-Doeuff, P. Deniard, S. Jobic. *Inorg. Chem.* 50 (2011) 8790 - 8796
- [2] C. D. Zhang, S. X. Liu, C. Y. Sun, F. J. Ma, and Z. M. Su. *Cryst. Growth Des.* 9 (2009) 3655 - 3660
- [3] S. Omwoma, C. T. Gore, Y. Ji, C. Hu, Y. F. Song, *Coord. Chem. Rev.* 286 (2015) 17 - 29
- [4] A. Bijelic, A. Rompel, *Coord. Chem. Rev.* 299 (2015) 22 - 38
- [5] H. Fujita, T. Fujita, T. Sakurai, Y. Seto. *Chemother.* 40 (1992) 173 - 178
- [6] C. L. Hill, J. Mole. *Catal A-Chem.* 262 (2007) 2 - 6
- [7] H. N. Miras, L. Vila`-Nadal, L. Cronin, *Chem. Soc. Rev.* 43 (2014), 5679 - 5699
- [8] R. Dessapt, M. Gabard, M. Bujoli-Doeuff. *Inorg. Chem.* 50 (2011) 8790 - 8796
- [9] L. Liu, H. M. Li, J. C. Dai. *Sci. China. Chem.* 57 (2014) 918 - 922
- [10] F. F. Jian, X. Wang, J. Wang, H. L. Xiao, R. R. Zhuang. *Polyhedron*, 29 (2010) 886 - 896
- [11] X. L. Hao, M. F. Luo, X. Wang, Y. G. Li, *Inorg. Chem. Commun.* 14 (2011) 1698 - 1702

- [12] H. Y. An, T. Q. Xu, H. Zheng, Z. B. Han, *Inorg. Chem. Commun.* 13 (2010) 302 - 305
- [13] C. H. Zhang, Y. G. Chen, S. X. Liu, *J. Solid State Chem.* 20 (2013) 80 - 85
- [14] S. Taleghani, M. Mirzaei, H. Eshtiagh-Hosseini, A. Frontera, *Coord. Chem. Rev.* 309 (2016) 84 - 106
- [15] Y. N. Chi, F.Y. Cui, A.R. Jia, X.Y. Ma, C.W. Hu, *Cryst. Eng. Comm.* 14 (2012) 3183 - 3188
- [16] X. L. Wang, H. L. Hu, A. X. Tian, *Cryst. Growth Des.* 10 (2010) 4786 - 4794
- [17] J. Niu, J. Hua, X. Ma, J. Wang, *Cryst. Eng. Comm.* 14 (2012) 4060 - 4067
- [18] S. R. Batten, N. R. Champness, X. M. Chen, J. Garcia-Martinez, S. Kitagawa, L. Öhrström, M. O’Keeffe, M. P. Suh, J. Reedijk, *Pure Appl. Chem.* 85 (2013) 1715 - 1724
- [19] Y. Q. Lan, S. L. Li, K. Z. Shao, X. L. Wang, Z. M. Su, *Dalton Trans.* (2008) 3824 - 3835
- [20] G. M. Sheldrick, *SADABS*, Germany, 1996.
- [21] G. M. Sheldrick, *SHELXS-97*, *Germany*, 1997
- [22] Y. Wang, L. Ye, T. G. Wang, X. B. Cui, S. Y. Shi, G. W. Wang, J. Q. Xu, *Dalton Trans.* 39 (2010) 1916 - 1919
- [23] C. H. Zhang, Y. G. Chen, S. X. Liu, *J. Solid State Chem.* 20 (2013) 80 - 85
- [24] H. Liu, L. Xu, G. G. Gao, F. Y. Li, Y. Y. Yang, *J. Solid State Chem.* 180 (2007) 1664–1671
- [25] S. Reinoso, P. Vitoria, J. M. Gutierrez-Zorrilla, L. Lezama, L. S. Felices, and J. I. Beitia, *Inorg. Chem.* 44 (2005) 9731 - 9742
- [26] X. K. Lin, Y. L. Wang, and L. X. Wu. *Langmuir*, 25 (2009) 6081 - 6087
- [27] L. B. Yang, Y. H. Shen, A. J. Xie, *J. Phys. Chem. C.* 111 (2007) 5300 - 5308
- [28] M. Sadakane, E. Steckhan, *Chem. Rev.* 98 (1998) 219 - 237
- [29] F. F. Jian, X. Wang, J. Wang, H. L. Xiao, R. R. Zhuang, *Polyhedron*, 29 (2010) 886 - 896
- [30] A. P. Brown, F. C. Anson, *Anal. Chem.* 49 (1997) 1589 - 1595

[31] E. B. Wang, Introduction of POMs, Beijing, 1997

Highlights

1. Two supramolecules are linked by covalent or non-covalent interactions
2. They are attributed to two representative models of supramolecule.
3. A rare multi-metal infinite supramolecular coordination polymer was formed.
4. They exhibit good catalytic activities for catalytic oxidation of methanol.

Graphical Abstracts

Two new organic-inorganic hybrid supramolecular complexes based on Co-EDTA, and Keggin polyanions have been successfully synthesized with different pH value by solution method. They are attributed to two representative models of supramolecule. Complex(1) is an infinite coordination polymer with a rare multi-metal structure of sodium-cobalt-containing, which is mainly linked through covalent bonds. Complex (2) is a normal supramolecule, which linked by non-covalent interactions of H-bonding interaction, electrostatic interaction and van der waals force.

Graphical Abstract Legend

